Approaching MIMO Capacity Using Bitwise Markov Chain Monte Carlo Detection

Rong-Rong Chen, Ronghui Peng, Alexei Ashikhmin, Behrouz Farhang-Boroujeny

***Abstract*—This paper examines near capacity performance of Markov Chain Monte Carlo (MCMC) detectors for multiple-input and multiple-output (MIMO) channels. The proposed MCMC detector (Log-MAP-tb b-MCMC) operates in a strictly bit-wise fashion and adopts Log-MAP algorithm with table look-up. When concatenated with an optimized low-density parity-check (LDPC) code, Log-MAP-tb b-MCMC can operate within 1.2-1.8 dB of the capacity of MIMO systems with 8 transmit/receive antennas at spectral efficiencies up to $\eta = 24$ bits/channel use (b/ch). This result improves upon best performance achieved by turbo coded systems using list sphere decoding (LSD) detector by 2.3-3.8 dB, leading to nearly 50% reduction in the capacity gap. Detailed comparisons of the Log-MAP-tb b-MCMC with LSD based detectors demonstrate that MCMC detector is indeed the detector of choice for achieving channel capacity both in terms of performance and complexity.**

***Index Terms*—MIMO detection, Markov chain Monte Carlo, list sphere decoding, LDPC codes, channel capacity.**

I. Introduction

MULTIPLE-INPUT multiple-output (MIMO) technologies have received much interests in the past decade because multiple antennas offer significant capacity gain for wireless channels [1]. As the number of transmit antenna increases, complexity of the optimum *maximum a posterior* (MAP) MIMO detector increases exponentially. This motivates the design of suboptimal MIMO detectors. Representative sub-optimum MIMO detectors include linear detectors such as minimum mean square error (MMSE) and zero-forcing (ZF) [2] detectors, the more sophisticated list sphere decoding (LSD) based detectors and its variants [3]–[5], and the recently proposed Markov Chain Monte Carlo (MCMC) detectors [6], [7]. The linear detectors achieve low computational complexity at the expense of significant performance loss. The LSD detectors have a complexity that grows exponentially with the number of transmit antenna [8]. The MCMC detector of [6] is a low-complexity MIMO detector that outperforms LSD detector [3] for turbo coded systems with a reduced complexity [7]. This paper examines performance of the MCMC detector operating at near channel capacity. Our main contributions are summarized as follows:

- Earlier versions of MCMC detectors operate in symbol-wise fashion ([6], [7], [9]). Later study has shown that a bit-wise implementation is more hardware friendly, which leads to significant complexity reduction [10]. However, no detailed study of bit-wise MCMC (b-MCMC) detector has been presented. We keep the focus of this paper on b-MCMC detectors and provide a detailed comparisons of b-MCMC versus symbol-wise MCMC (s-MCMC). It is shown that the low-complexity implementation of b-MCMC is sufficient to achieve the desirable near capacity performance.
- The studies in [3], [4], [6], [7], [9], [10] are limited to Max-Log MIMO detectors. In this work we propose a novel bit-wise MCMC detector that employs the Log-MAP algorithm with table look-up (Log-MAP-tb). The Log-MAP-tb b-MCMC detector is found to achieve superior performance over the Max-Log b-MCMC detector at reduced complexity.
- We show that Log-MAP-tb b-MCMC is amicable for channel code optimization. The extrinsic information transfer (EXIT) chart approach for optimizing low-density parity-check (LDPC) codes (originally proposed for optimal MAP detectors, [11]) leads to effective channel codes for the MCMC detector.
- We obtain unprecedent near capacity performance at high spectral efficiencies by using Log-MAP-tb b-MCMC in conjunction with the LDPC codes that we design. When operating at near the capacity, the complexity of the MCMC detector remains orders of magnitude less than LSD detectors. Our study also covers a comparison of several LSD based detectors that have been reported in the literature, but never been compared against each other.

II. System Model

We consider a MIMO channel with t transmit and r receive antennas. The channel model is given by :

$$\mathbf{y} = \sqrt{\frac{\rho}{t}}\mathbf{H}\mathbf{d} + \mathbf{n}, \tag{1}$$

where $\mathbf{d} \in \mathbb{C}^t$, $\mathbf{y} \in \mathbb{C}^r$, and $\mathbf{n} \in \mathbb{C}^r$ are complex column vectors that represent the transmitted signal, received signal, and channel noise, respectively; $\mathbf{H}$ is the r by t channel fading matrix with independent and identically distributed (i.i.d.) complex Gaussian $\mathcal{CN}(0,1)$ distributed entries; $\mathbf{H}$ is also assumed to be independent over time; the noise vector $\mathbf{n}$ has i.i.d. $\mathcal{CN}(0,1)$ distributed entries; ρ denotes the SNR per receive antenna. In this paper, we assume that the ideal channel

Paper approved by T. M. Duman, the Editor for Coding Theory and Applications of the IEEE Communications Society. Manuscript received October 13, 2008; revised June 19, 2009 and August 18, 2009.

R.-R. Chen, R. Peng, and B. Farhang-Boroujeny are with the Dept. of Electrical and Computer Engineering, Univ. of Utah, 50 S. Central Campus Dr. Rm. 3280, Salt Lake City, UT, 84112 USA (e-mail: {rchen, peng, farhang}@ece.utah.edu).

A. Ashikhmin is with Bell Laboratories, Alcatel-Lucent, 600 Mountain Ave, Murray Hill, NJ 07974, USA (e-mail: aea@alcatel-lucent.com).

This work is supported in part by NSF under grant ECS-0547433 and ECS-0524720.

The material in this paper was presented in part at the 6th IEEE Workshop on Signal Processing Advances in Wireless Communication (SPAWC'05).

Digital Object Identifier 10.1109/TCOMM.2010.02.080533

0090-6778/10$25.00 © 2010 IEEE

Authorized licensed use limited to: The University of Utah. Downloaded on February 23,2010 at 00:23:03 EST from IEEE Xplore. Restrictions apply.

state information is available at the receiver. At the transmitter, a sequence of information bit is passed to a channel encoder. The coded bit sequence is then mapped to a sequence of complex symbols through Gray mapping. The size of the constellation is $M = 2^{M_c}$. The symbol sequence is then divided into blocks of t symbols and sent through t transmit antennas over the MIMO channel. At the receiver, the turbo principle [12] is applied to perform joint MIMO detection and channel decoding.

III. Bit-Wise MCMC Detector Based on Log-MAP with Table Look-Up

In this section, we describe the proposed Log-MAP-tb b-MCMC detector. Compared to prior work on symbol-wise MCMC detection [6], [7], [9], [13], Log-MAP-tb b-MCMC operates in a strictly bit-wise fashion, hence is amicable for efficient circuit implementation [10]. Furthermore, we show that the use of Log-MAP-tb yields better performance and lower complexity than existing Max-Log detectors [6], [7], [9].

A. Bit-wise Gibbs Sampler

The MCMC detector operates in two steps: It first adopts a statistical procedure called the Gibbs sampler (GS) to produce a small sample set containing the most likely transmitted vectors. Subsequently, these vectors are used to compute output bit-wise log-likelihood ratio (LLRs) to be passed to the channel decoder. We first introduce some notations. Let $\mathbf{d} = (d_1, \cdots, d_t)^T$ represent the transmitted signal vector, where d_j is the complex symbol transmitted from the j-th antenna. The notation $(\cdot)^T$ denotes the transpose operator. The bit sequence corresponding to $\mathbf{d} = (d_1, \cdots, d_t)^T$ is denoted by $\mathbf{b} = (b_1, b_2, \cdots, b_K)^T$, where $K = tM_c$. Given the received signal vector $\mathbf{y} = (y_1, \cdots, y_r)^T$ and the LLR of the i-th bit provided by the channel decoder, denoted by λ_i, the GS performs I iterations described as below to identify a sample set containing I most likely transmitted bit vectors $\{\mathbf{b}^{(n)}, n = 1, \cdots I\}$.

Bit-wise Gibbs Sampler

Initialization $n = 0$;

generate the initial vector $\mathbf{b}^{(0)} = \{b_1^{(0)}, \cdots, b_K^{(0)}\}$ randomly.

for $n = 1$ to I

for $i = 1$ to K

First compute γ_i, the LLR of the i-th bit of $\mathbf{b}^{(n)}$ according to its *a posteriori* probability distribution conditioned upon $\mathbf{y}, \lambda_i$ and $\left(b_1^{(n)}, \cdots, b_{i-1}^{(n)}, b_{i+1}^{(n-1)}, \cdots, b_K^{(n-1)}\right)^T$:

$$\gamma_i = \ln\left[\frac{P(b_i^{(n)} = 1 | b_1^{(n)}, \cdots, b_{i-1}^{(n)}, b_{i+1}^{(n-1)}, \cdots, b_K^{(n-1)}, \mathbf{y}, \lambda_i)}{P(b_i^{(n)} = -1 | b_1^{(n)}, \cdots, b_{i-1}^{(n)}, b_{i+1}^{(n-1)}, \cdots, b_K^{(n-1)}, \mathbf{y}, \lambda_i)}\right]. \quad (2)$$

Generate a random number U uniformly between $[0, 1]$. If $U < 1/(1 + \exp(-\gamma_i))$, let

$b_i^{(n)} = 1$, otherwise let $b_i^{(n)} = -1$.

end i loop

end n loop

Let $\mathbf{d}^+$ and $\mathbf{d}^-$ denote signal vectors corresponding to $\left(b_1^{(n)}, \cdots, b_{i-1}^{(n)}, +1, b_{i+1}^{(n-1)}, \cdots, b_K^{(n-1)}\right)^T$ and $\left(b_1^{(n)}, \cdots, b_{i-1}^{(n)}, -1, b_{i+1}^{(n-1)}, \cdots, b_K^{(n-1)}\right)^T$, respectively. We can compute (2) as

$$\begin{aligned}\gamma_i &= \left\|\mathbf{y} - \sqrt{\frac{\rho}{t}}\mathbf{H}\mathbf{d}^-\right\|^2 - \left\|\mathbf{y} - \sqrt{\frac{\rho}{t}}\mathbf{H}\mathbf{d}^+\right\|^2 + \lambda_i \\ &= \left(\|d_j^-\|^2 - \|d_j^+\|^2\right)\rho_{jj} + 2\,\mathrm{Re}\left[(d_j^+ - d_j^-)^*\left(v_j - \sum_{l \neq j}\rho_{jl} d_l^+\right)\right] \\ &\quad + \lambda_i, \end{aligned} \quad (3)$$

where $(\cdot)^*$ denotes the Hermitian operator, $j = \lceil i/M_c \rceil$ is the index of the symbol that bit i is mapped to, d_j^+, d_j^- denote the j-th symbol of $\mathbf{d}^+$ and $\mathbf{d}^-$, $v_j = \sqrt{\frac{\rho}{t}}\,\mathbf{h}_j^*\,\mathbf{y}$, where $\mathbf{h}_j$ is the j-th column of $\mathbf{H}$, and $\rho_{jl} = \frac{\rho}{t}\,\mathbf{h}_j^*\,\mathbf{h}_l$.

B. Complexity comparison of bit-wise Gibbs sampler and symbol-wise Gibbs sampler

As opposed to the bit-wise GS described in III-A, symbol-wise GS has been widely used in the literature for higher order modulations [7], [9], [13]. At each iteration of the symbol-wise GS, a complex symbol is generated randomly according to the *a posteriori* symbol probability distribution π. Compared to the bit-wise GS where each bit is generated sequentially according to its LLR γ_i, the symbol-wise GS generates each group of M_c bits (constituting the same complex symbol) simultaneously. Computation of π involves evaluations of $M = 2^{M_c}$ terms of the form $\left\|\mathbf{y} - \sqrt{\frac{\rho}{t}}\mathbf{H}\mathbf{x}^{(k)}\right\|^2$, where $\{\mathbf{x}^{(k)}, k = 1, \cdots, M\}$ differs only in one symbol. Hence, the complexity of the symbol-wise GS is about M/M_c times that of the bit-wise GS.

C. Computations of LLRs using Max-Log and Log-MAP-tb

Following the bit-wise GS described in III-A, we compute the output LLRs also in a strictly bit-wise fashion. This differs from the symbol-wise computations presented in [7], [9] due to the use of symbol-wise GS. We first run the bit-wise GS over I iterations to generate vectors $\mathbf{b}^{(1)}, \cdots, \mathbf{b}^{(I)}$ which are put into a set $\mathcal{B}$. Following [6], we run Q parallel GS to obtain more samples and they are all added (except for repetitions) to $\mathcal{B}$. For each bit i, we introduce an expanded set $\mathcal{B}_i^e$ that contains all the vectors in $\mathcal{B}$, as well as vectors that differ from the vectors in $\mathcal{B}$ only in bit i. We let $\mathcal{B}_{i,+1}^e$ and $\mathcal{B}_{i,-1}^e$ denote the set of bit vectors in $\mathcal{B}_i^e$ whose i-th bit is $+1$ and -1, respectively. Considering $\mathcal{B}^e$ instead of $\mathcal{B}$ assures that the number of elements in $\mathcal{B}_{i,+1}^e$ and $\mathcal{B}_{i,-1}^e$ are the same. This is necessary for successful operation of the various Max-Log and Log-MAP detectors studied in this paper.

The Max-Log algorithm is used extensively in the literature to compute the output LLRs for a given MIMO detector [3]–[7]. The Max-Log b-MCMC detector utilizes $\mathcal{B}_i^e$ to compute the extrinsic output LLR for the i-th bit using the Max-Log approximation

$$\begin{aligned}\mathrm{LLR}_i &= \ln\frac{P(b_i = 1|\mathbf{y}, \boldsymbol{\lambda})}{P(b_i = -1|\mathbf{y}, \boldsymbol{\lambda})} \\ &\approx \max_{\{\mathbf{b}:\, \mathbf{b} \in \mathcal{B}_{i,+1}^e\}}\left\{-\left\|\mathbf{y} - \sqrt{\frac{\rho}{t}}\mathbf{H}\mathbf{d}(\mathbf{b})\right\|^2 + \frac{1}{2}\boldsymbol{\lambda}^T\mathbf{b}\right\} \\ &\quad - \max_{\{\mathbf{b}:\, \mathbf{b} \in \mathcal{B}_{i,-1}^e\}}\left\{-\left\|\mathbf{y} - \sqrt{\frac{\rho}{t}}\mathbf{H}\mathbf{d}(\mathbf{b})\right\|^2 + \frac{1}{2}\boldsymbol{\lambda}^T\mathbf{b}\right\} - \lambda_i \end{aligned} \quad (4)$$

Authorized licensed use limited to: The University of Utah. Downloaded on February 23,2010 at 00:23:03 EST from IEEE Xplore. Restrictions apply.

where $\boldsymbol{\lambda} = (\lambda_1, \cdots, \lambda_K)^T$ denotes the LLR from the channel decoder and $\mathbf{d}(\mathbf{b})$ denotes the symbol vector corresponding to the bit vector $\mathbf{b}$.

The proposed Log-MAP-tb b-MCMC detector is obtained by replacing Max-Log in (4) with the more accurate Log-MAP-tb [14]. If we use the same $\mathcal{B}^e_{i,+1}$ and $\mathcal{B}^e_{i,-1}$, Log-MAP-tb indeed has a higher complexity than Max-Log. However, we find that Log-MAP-tb can achieve better performance than Max-Log while requiring a much smaller sample set $\mathcal{B}$. This leads to reduction in overall complexity. We confirm this observation through simulation results in Section V.

IV. EXIT Charts and LDPC Code Design

We first compare the performance of various detectors using EXIT chart. Besides MCMC detectors, four versions of LSD based detectors are considered including the Max-Log LSD [3], the Max-Log soft-in and soft-out (SISO) LSD [4], and our modified versions of these two detectors using Log-MAP-tb, denoted by Log-MAP-tb LSD and Log-MAP-tb SISO-LSD. For the LSD based detectors, tree search algorithms are applied to find a list $\mathcal{L}$ containing likely samples. In order to apply Log-MAP-tb, it is necessary to consider an expanded list $\mathcal{L}^e$ (similar to $\mathcal{B}^e$ defined in Section III-C for MCMC) when computing output LLRs.

We consider a TX8 16QAM system using 8 transmit and 8 receive antenna and 16QAM modulation. Fig. 1 presents the EXIT curves of six detectors at $E_b/N_0 = 4.1$ dB (where the definition of E_b/N_0 follows [3]). For the 10x10 Log-MAP-tb b-MCMC (10x10 indicates $Q = 10$ parallel GS and $I = 10$ iterations for each GS), the number of samples in $\mathcal{B}$ equals $Q \cdot I = 100$. Hence, to ensure fair comparison, we let $L = 100$ (L is the number of samples in $\mathcal{L}$) for both Log-MAP-tb LSD and Log-MAP-tb SISO-LSD. We follow [3] and [4] to choose $L = 512$ for Max-Log LSD and Max-Log SISO-LSD. In general, the higher an EXIT curve, the better the detector performance. This is independent of the choice of channel codes. Fig. 1 shows that the EXIT curve of 10x10 Log-MAP-tb b-MCMC is the highest among all detectors, which is consistent with the simulation results (see Fig. 4). The effectiveness of the Log-MAP-tb over Max-Log is also shown in Fig. 1. Albeit requiring four times the number of samples, the EXIT curve of 20x20 Max-Log b-MCMC is lower than that of the 10x10 Log-MAP-tb b-MCMC. Similar observations hold for the LSD based detectors. Next, we adopt the EXIT chart method [11] to optimize the LDPC code for the 10x10 Log-MAP-tb b-MCMC. We first generate the detector EXIT curve at $E_b/N_0 = 4.1$ dB (slightly above the channel capacity for a rate $1/2$ code), shown as the top curve in Fig. 1. Under specific code design constraints, we find an optimized LDPC code (C1) by applying linear programming techniques to match the EXIT curve of the code with the EXIT curve of the detector. The code constraints used in our numerical search and the resulting optimized parameters of C1 are given in Section V. We have also attempted to apply the EXIT chart approach to optimize LDPC codes for other detectors. Results of such design, however, are not satisfactory. For instance, we observe that the code specifically designed for the Log-MAP-tb SISO-LSD using the EXIT chart approach yields an inferior performance to that of C1, when both codes are applied

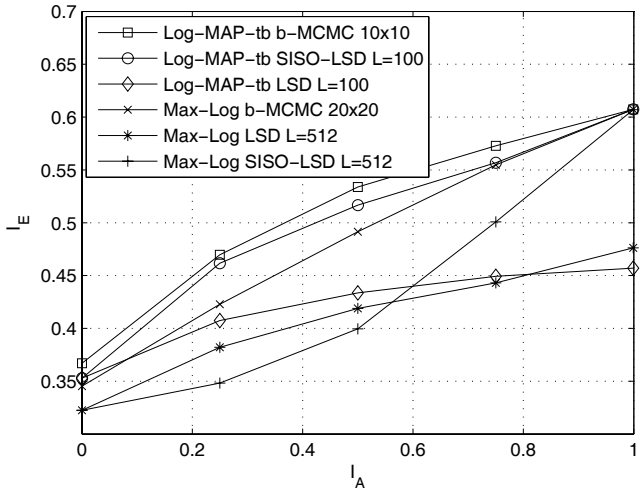

Fig. 1. EXIT curves of various detectors at $E_b/N_0 = 4.1$ dB for a TX8 16QAM system.

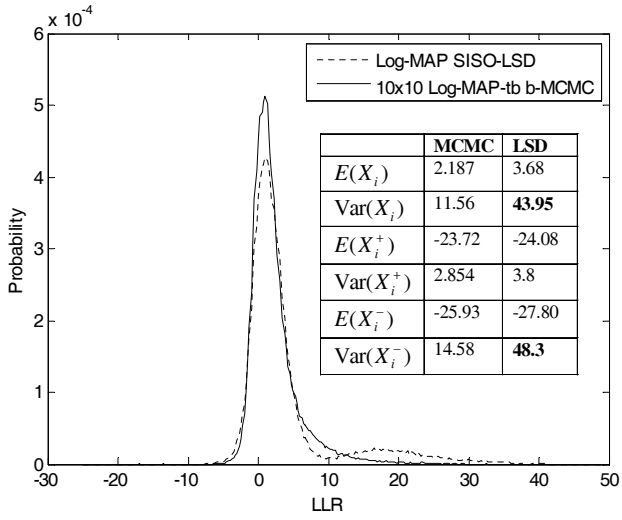

	MCMC	LSD
$E(X_i)$	2.187	3.68
$\mathrm{Var}(X_i)$	11.56	**43.95**
$E(X_i^+)$	-23.72	-24.08
$\mathrm{Var}(X_i^+)$	2.854	3.8
$E(X_i^-)$	-25.93	-27.80
$\mathrm{Var}(X_i^-)$	14.58	**48.3**

Fig. 2. Probability distribution of the output LLR of 10x10 Log-MAP-tb b-MCMC and Log-MAP-tb SISO-LSD at $E_b/N_0 = 4.1$ dB for a TX8 16QAM system.

to a MIMO system using the *same* Log-MAP-tb SISO-LSD detector. We conjecture that this is due to both the inaccuracy of the EXIT chart design method and the discrepancy in detection performance. To see this, we compare the output LLR distribution of the 10x10 Log-MAP-tb b-MCMC and the Log-MAP-tb SISO-LSD ($L = 100$). In Fig. 2, conditioned upon a transmitted bit $b_i = +1$, we plot the probability density function (pdf) of the extrinsic LLR, denoted by X_i, generated at the output of these two detectors, assuming uniform prior. The mean and variances of X_i are also given in Fig. 2. We observe from Fig. 2 that there is a peak around LLR=18 for the SISO-LSD, which is not present for the MCMC. The SISO-LSD also has a larger variance $\mathrm{Var}(X_i) = 43.95$ compared to $\mathrm{Var}(X_i) = 11.56$ for the MCMC. These suggest that the SISO-LSD is more likely to over estimate output LLRs, thus causing degradation in decoding performance. This provides a good explanation as to why the EXIT chart-based code design is less effective for the SISO-LSD.

To better understand the root of such differences in the

Authorized licensed use limited to: The University of Utah. Downloaded on February 23,2010 at 00:23:03 EST from IEEE Xplore. Restrictions apply.

output statistics, we recall that X_i is computed via the Log-MAP algorithm

$$X_i = \ln \frac{P(b_i = 1|\mathbf{y}, \boldsymbol{\lambda})}{P(b_i = -1|\mathbf{y}, \boldsymbol{\lambda})}$$
$$\approx \ln \sum_{\{\mathbf{b}:\, \mathbf{b} \in \mathcal{B}^e_{i,+1}\}} \exp\Big\{ -\Big\|\mathbf{y} - \sqrt{\frac{\rho}{t}}\mathbf{H}\mathbf{d}(\mathbf{b})\Big\|^2 + \frac{1}{2}\boldsymbol{\lambda}^T\mathbf{b}\Big\}$$
$$- \ln \sum_{\{\mathbf{b}:\, \mathbf{b} \in \mathcal{B}^e_{i,-1}\}} \exp\Big\{ -\Big\|\mathbf{y} - \sqrt{\frac{\rho}{t}}\mathbf{H}\mathbf{d}(\mathbf{b})\Big\|^2 + \frac{1}{2}\boldsymbol{\lambda}^T\mathbf{b}\Big\} - \lambda_i. \quad (5)$$

We denote the first logarithmic term in (5) by X_i^+ and the second term by X_i^-. Note that while $\mathrm{Var}(X_i^+)$ are close for these two detectors, the difference in $\mathrm{Var}(X_i^-)$ is significant. Given $b_i = +1$, it is more challenging to identify significant samples that contribute to X_i^- than those contribute to X_i^+. The stochastic nature of the b-MCMC makes it a good detector for estimating both X_i^+ and X_i^-. In comparison, the SISO-LSD is inferior in estimating X_i^-, thus yielding LLRs that are overconfident. A possible approach to alleviate this problem for the SISO-LSD is to scale down the LLR appropriately or to saturate it to a fixed value, before feeding it to the channel decoder [15].

In a related work [16], limitations of the EXIT chart approach for LSD based detectors are studied for small MIMO systems. It points out the inaccuracy of the EXIT curves for these detectors and shows that better codes can be obtained by performing code design using EXIT curves of more sophisticated LSD based detectors. This observation is consistent with our finding: a code designed for a superior detector (the b-MCMC detector in our case) may enable better performance for an inferior detector than a code specifically designed for the latter detector. An in-depth investigation into this issue, however, is beyond the scope of this paper.

We have also obtained an optimized LDPC code, C2, for a TX8 64QAM system using the EXIT curve of the 10x10 Log-MAP-tb b-MCMC detector at $E_b/N_0 = 6.6$ dB. This turns out to be a good code for the 20x20 Max-Log b-MCMC. For the Log-MAP-tb SISO-LSD, since the detection complexity increases exponentially with decreasing SNR, the simulation time of this detector becomes orders of magnitudes longer compared to that of the Log-MAP-tb b-MCMC at operating SNRs that are about 2 dB above capacity. This prohibits feasible code design for the Log-MAP-tb SISO-LSD and also makes it difficult to obtain reliable performance curve for this detector in the near capacity region.

V. Simulation Results

In this section, we present simulation results to compare performance of MCMC detectors and four versions of LSD based detectors described in Section IV. While Max-Log LSD and Max-Log SISO-LSD are proposed separately in [3] and [4], a direct comparison between these two detectors in performance and complexity seems to be missing in the literature. Here we provide a systematic comparison of these two detectors, together with their modified versions against MCMC detectors. All the channel codes used here have a rate of $R = 1/2$ and a code length of 18432. The turbo code we use is the same as that of [3]. The optimized LDPC codes C1 and C2 (parameters are given in captions of Fig. 4 and Fig. 5) are used for the TX8 16QAM and TX8 64QAM system, respectively.

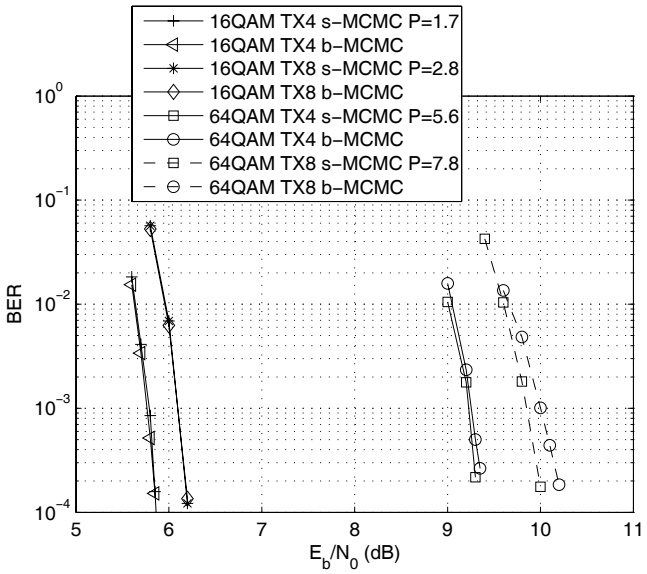

Fig. 3. Comparisons of Max-Log b-MCMC versus Max-Log s-MCMC in performance and complexity. Replacing b-MCMC by s-MCMC in the same system leads to a P-fold increase in simulation time.

A. Max-Log b-MCMC versus Max-Log s-MCMC

We first compare performance of Max-Log b-MCMC and Max-Log s-MCMC [6]. The Max-Log b-MCMC employs a bit-wise GS as described in Section III-A and the LLRs are computed using Max-Log (4). The Max-Log s-MCMC employs a symbol-wise MCMC and the LLRs are computed following [6] using symbol-wise expanded sets. We examine four turbo coded systems: TX4 16QAM, TX4 64QAM, TX8 16QAM and TX8 64QAM. For each system, the same parameters Q and I are used for both b-MCMC and s-MCMC. We use 10x10 ($Q = I = 10$) for the TX4 16QAM system, 20x20 for the other three systems. Fig. 3 shows that these two detectors perform very closely. It is only for the TX8 64QAM system that the s-MCMC performs slightly better than b-MCMC by about 0.2 dB. Replacing b-MCMC by s-MCMC increases the simulation time of each system by a factor of P, where P varies from 1.7 to 7.8. This confirms that b-MCMC achieves similar performance as s-MCMC with much reduced complexity.

B. TX8 16QAM system

Performance of various detectors for a TX8 16QAM system is shown in Fig. 4. The LDPC code C1 is used for 10x10 Log-MAP-tb b-MCMC, 20x20 Max-Log b-MCMC, and Log-MAP-tb SISO-LSD ($L = 100$) because it gives the best performance (among the codes we have tested) for each of these detectors. The parameter G denotes the normalized simulation time of each system against the LDPC coded system that employs 10x10 Log-MAP-tb b-MCMC. For each system, the simulation time is recorded at a SNR point with

Authorized licensed use limited to: The University of Utah. Downloaded on February 23,2010 at 00:23:03 EST from IEEE Xplore. Restrictions apply.

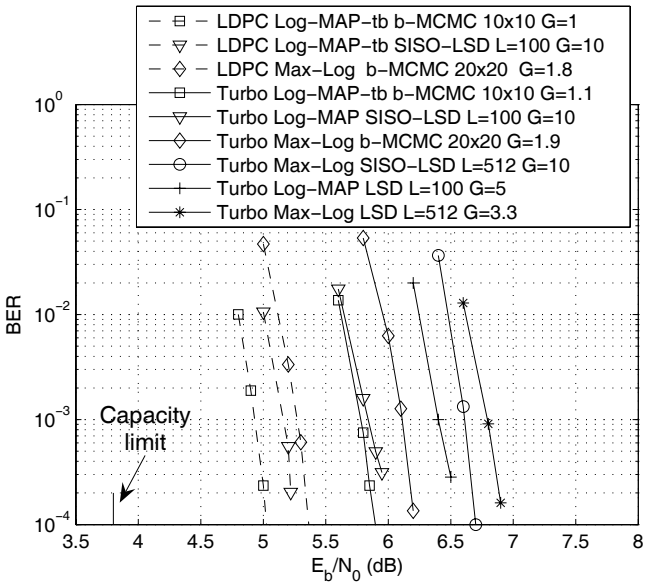

Fig. 4. Performance of turbo and LDPC coded TX8 16QAM systems. The optimized LDPC code C1 is found using the EXIT chart approach to best match the 10x10 Log-MAP-tb b-MCMC. The parameters are given by $d_c = 5$, $d_v = [2, 3, 11, 12]$, $u_v = [0.65, 0.33, 0.01, 0.005]$, where d_c is the degree of check nodes, d_v is the degree sequence of variable nodes, $u_v(i)$ is the fraction of variables nodes that have degree $d_v(i)$. The code rate is $1/2$ and the code length is 18432. The code design constraints that we assume are: the maximum check node degree satisfies $d_c \leq 7$ and the maximum variable node degree satisfies $d_v \leq 200$.

BER $\approx 10^{-4}$. Main findings from Fig. 4 are summarized as follows:

(a) For both turbo coded and LDPC coded systems, the same Log-MAP-tb b-MCMC detector gives the best performance with the lowest complexity. Its simulation time $G \approx 1$ is much shorter compared to LSD based detectors $G = 3.3 \sim 10$. While the Max-Log LSD runs the fastest among LSD-based detectors, it performs nearly 2 dB worse than the LDPC coded Log-MAP-tb b-MCMC and is about three times slower.

(b) The EXIT chart code design is effective for Log-MAP-tb b-MCMC. The optimized code C1 performs about 1 dB better than the turbo coded system.

(c) The 10x10 Log-MAP-tb b-MCMC outperforms 20x20 Max-Log b-MCMC by $0.3 \sim 0.4$ dB with about half the simulation time.

(d) With the same list size, Max-Log SISO-LSD performs about 0.3 dB better than Max-Log LSD. Its simulation time, however, is three times longer because it needs to re-generate $\mathcal{L}$ for each iteration of channel decoding and MIMO detection.

(e) With $L = 100$, Log-MAP-tb SISO-LSD outperforms Log-MAP-tb LSD, albeit at twice the simulation time. Since Log-MAP-tb LSD uses a fixed $\mathcal{L}$ over all iterations, it requires a larger list to get good performance. In comparison, since Log-MAP-tb SISO-LSD adaptively finds $\mathcal{L}$ using priors, a small list size $L = 100$ suffices.

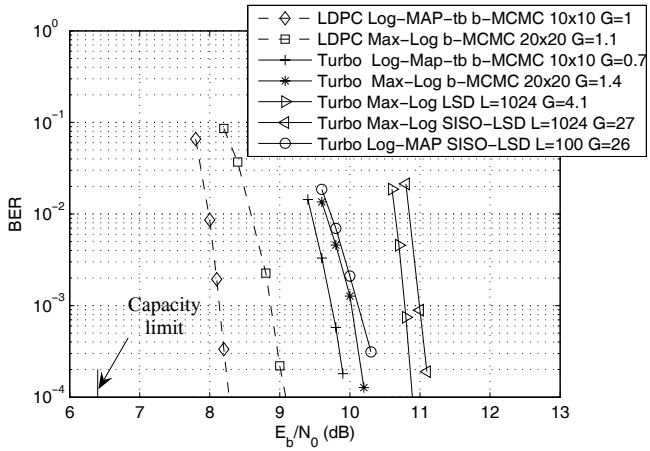

Fig. 5. Performance of turbo and LDPC coded TX8 64QAM systems. The optimized LDPC code C2 is found using the EXIT chart approach to best match the 10x10 Log-MAP-tb b-MCMC. Parameters of C2 are given by $d_c = 5$, $d_v = [2, 3, 8, 9]$, $u_v = [0.66, 0.31, 0.02, 0.01]$. The code rate is $1/2$ and the code length is 18432. The code design constraints that we assume are: the maximum check node degree satisfies $d_c \leq 7$ and the maximum variable node degree satisfies $d_v \leq 200$.

C. TX8 64QAM system

For the TX8 64QAM system, as shown in Fig. 5, the same 10x10 Log-MAP-tb b-MCMC detector still gives the best near capacity performance with the lowest complexity. Its simulation time is $G = 0.7 \sim 1$ whereas LSD based detectors (operating at SNRs that are 2 dB higher) require $G = 4.1 \sim 27$. Due to the exponential complexity of LSD based detectors, it becomes computationally infeasible to operate these detectors in the lower SNR region. The LDPC code optimization is shown to be effective for Log-MAP-tb b-MCMC, yielding a 1.8 dB coding gain over the turbo coded system. The 10x10 Log-MAP-tb b-MCMC is about 1 dB better than the 20x20 Max-Log b-MCMC with comparable simulation time, thus confirming the superiority of the Log-MAP-tb over Max-Log in both performance and complexity.

D. Performance Summary

A summary of the performance comparison between this work, [3], and [6] is given in Table I for the TX8 16QAM and 64QAM systems. We compare both the capacity gap and the number of samples used for MIMO detection. The number of samples equals the list size L for LSD based detectors and equals $Q \cdot I$ for MCMC detectors. As shown in Table I, this work reduces the capacity gap and number of samples significantly. For the TX8 64QAM system, capacity gap is reduced from 4 dB [6] to 1.8 dB and the number of samples is reduced from 900 to 100. Both the Log-MAP-tb b-MCMC detector and LDPC code optimization contribute to this performance gain.

VI. Conclusion

This paper studies performance of MCMC detection in the near capacity regime. The proposed Log-MAP-tb b-MCMC detector has two distinguished features. (1) It adopts a strictly bit-wise implementation that enables complexity

Authorized licensed use limited to: The University of Utah. Downloaded on February 23,2010 at 00:23:03 EST from IEEE Xplore. Restrictions apply.

TABLE I
COMPARISONS OF CAPACITY GAP AND NUMBER OF SAMPLES REQUIRED FOR MIMO DETECTION.

System	Spectral efficiency	Capacity limit		results in [3]	results in [6]	this work
TX8 16QAM	16 b/ch	3.8 dB	capacity gap (dB)	3.7	2.6	**1.4**
			# of samples	512	400	**100**
TX8 64QAM	24 b/ch	6.4 dB	capacity gap (dB)	5.6	4	**1.8**
			# of samples	1024	900	**100**

[3] considers turbo coded systems with Max-Log LSD, [6] considers turbo coded systems with Max-Log s-MCMC detection, and this work considers LDPC coded systems with Log-MAP-tb b-MCMC.

reduction from existing symbol-wise MCMC detectors. (2) It adopts Log-MAP-tb to overcome performance limitations of existing Max-Log MCMC detectors. The Log-MAP-tb b-MCMC detector in conjunction with LDPC code optimization yields unprecedent near capacity performance at high spectral efficiencies of $16 \sim 24$ b/ch. As summarized in Table I, our results not only significantly improve the best performance achieved by the turbo coded systems with the LSD detector by 2.3-3.8 dB, but also outperform existing work on Max-Log MCMC by 1.2-2.2 dB. Furthermore, the best near capacity performance of the Log-MAP-tb b-MCMC is obtained with a simulation time that is much less than that of the LSD based detectors and the Max-Log MCMC. This work strongly established the proposed MCMC detector as the detector of choice for approaching MIMO channel capacity.

REFERENCES

[1] E. Telatar, "Capacity of multi-antenna gaussian channels," *European Trans. Telecommun.*, vol. 10, no. 6, pp. 585-595, Nov.-Dec. 1999.

[2] G. Foschini, "Layered space-time architecture for wireless communication in a fading environment when using multi-element antennas," *Bell Labs Tech. J.*, vol. 1, no. 2, pp. 41-59, Aug. 1996.

[3] B. M. Hochwald and S. ten Brink, "Achieving near-capacity on a multiple-antenna channel," *IEEE Trans. Commun.*, vol. 51, no. 3, pp. 389-399, Mar. 2003.

[4] H. Vikalo, B. Hassibi, and T. Kailath, "Iterative decoding for MIMO channels via modified sphere decoding," *IEEE Trans. Wireless Commun.*, vol. 3, no. 6, pp. 2299-2311, Nov. 2004.

[5] R. Wang and G. B. Giannakis, "Approaching MIMO channel capacity with soft detection based on hard sphere decoding," *IEEE Trans. Commun.*, vol. 54, no. 4, Apr. 2006.

[6] B. Farhang-Boroujeny, H. Zhu, and Z. Shi, "Markov Chain Monte Carlo techniques for CDMA and MIMO communication systems," *IEEE Trans. Signal Process.*, vol. 54, no. 5, pp. 1896-1909, May 2006.

[7] H. Zhu, B. Farhang-Beroujeny, and R. R. Chen, "On performance of sphere decoding and Markov Chain Monte Carlo methods," *IEEE Signal Process. Lett.*, vol. 12, no. 10, pp. 669-672, Oct. 2005.

[8] J. Jalden and B. Ottersten, "On the complexity of sphere decoding in digital communications," *IEEE Trans. Signal Process.*, vol. 53, no. 4, pp. 1474-1484, 2005.

[9] R.-R. Chen, B. Farhang-Boroujeny, and A. Ashikhmin, "Capacity-approaching LDPC codes based on Markov Chain Monte Carlo MIMO detection," in *Proc. IEEE 6th. Workshop Signal Process. Advances Wireless Commun. SPAWC'05*, NY, 2005, pp. 285-288.

[10] S. A. Laraway and B. Farhang-Boroujeny, "Implementation of a Markov Chain Monte Carlo based multiuser/MIMO detector," *IEEE Trans. Circuits Syst.*, 2008.

[11] S. ten Brink, G. Kramer, and A. Ashikhmin, "Design of low-density parity-check codes for modulation and detection," *IEEE Trans. Commun.*, vol. 52, no. 4, pp. 670-678, Apr. 2004.

[12] J. Hagenauer, "The turbo principle: tutorial introduction and state of art," in *Proc. Int. Symp. Turbo-codes Related Topics*, Brest, France, Sept. 1997, pp. 1-11.

[13] A. Doucet and X. Wang, "Monte Carlo methods for signal processing," *IEEE Signal Process. Mag.*, vol. 22, no. 6, pp. 152-170, Nov. 2005.

[14] P. Robertson, E. Villebrun, and P. Hoeher, "A comparison of optimal and sub-optimal MAP decoding algorithms operating in the log domain," in *Proc. IEEE Int. Conf. Commun.*, vol. 2, Seattle, June 1995, pp. 1009-1013.

[15] A. Elkhazin, K. N. Plataniotis, and S. Pasupathy, "Reduced-dimension MAP turbo-blast detection," *IEEE Trans. Commun.*, vol. 54, no. 1, pp. 108-118, Jan. 2006.

[16] F. Vazquez-Araujo, M. Gonzalez-Lopez, and L. Castedo, "Exit functions of soft iterative MIMO detectors and their application to capacity-approaching coding," in *IEEE Int. Conf. Acoustics, Speech Signal Process. (ICASSP'2007).*

Authorized licensed use limited to: The University of Utah. Downloaded on February 23,2010 at 00:23:03 EST from IEEE Xplore. Restrictions apply.